

# DEEP AUTO-ENCODER NETWORK FOR HYPERSPECTRAL IMAGE UNMIXING

Yuanchao Su<sup>1</sup>, Jun Li<sup>1</sup>, Antonio Plaza<sup>2</sup>, Andrea Marinoni<sup>3</sup>, Paolo Gamba<sup>3</sup>, and Yuancheng Huang<sup>4</sup>

<sup>1</sup>Guangdong Key Laboratory for Urbanization and Geo-Simulation,

School of Geography and Planning, Sun Yat-sen University, Guangzhou, 510275, China.

<sup>2</sup>Hyperspectral Computing Laboratory, Department of Technology of Computers and Communications, Escuela Politécnica, University of Extremadura, Cáceres, E-10071, Spain.

<sup>3</sup>Dipartimento di Ingegneria Industriale e dell'Informazione, Università degli Studi di Pavia, Pavia, I-27100, Italy.

<sup>4</sup>College of Geomatics, Xi'an University of Science and Technology, Xi'an, 710054, China.

## ABSTRACT

In this paper, we propose a deep auto-encoder network for the unmixing for hyperspectral data with outliers and low signal to noise ratio. The proposed deep auto-encoder network composes of two parts. The first part of the network adopts stacked non-negative sparse auto-encoder to learn the spectral signatures such that to generate a good initialization for the network. In the second part of the network, a variational auto-encoder is employed to perform unmixing, aiming at the endmember signatures and abundance fractions. The effectiveness of the proposed method is verified by using a synthetic data set. In our comparison with other state-of-the-art unmixing methods, the proposed approach demonstrates highly competitive performance.

**Index Terms**— Hyperspectral unmixing, Non-negative sparse auto-encoder, Variational auto-encoder, Deep learning

## 1. INTRODUCTION

Due to the relatively low-spatial resolution of hyperspectral images, many pixels would be mixed by several materials, which brings difficulty for the characterization of hyperspectral data and might lead to dramatic inaccuracy in the understanding and quantification the considered scenes. In order to deal with mixed pixels, many blind unmixing algorithms have been developed using different criteria, such as N-FINDR [1], vertex component analysis (VCA) [2], minimum volume constrained nonnegative matrix factorization (MVC-NMF)[3], minimum volume simplex analysis (MVSA)[4], robust collaborative nonnegative matrix factorization (R-CoNMF)[5], Bayesian approaches [6], piece-wise

---

This work was supported by National Natural Science Foundation of China under Grant 61771496, National Key Research and Development Program of China under Grant 2017YFB0502900, Guangdong Provincial Natural Science Foundation under Grant 2016A030313254.

convex multiple-model (PCOMMEND)[7] and many others [8, 9]. Although these methods exhibit outstanding performance in unmixing, they are with limitations when the data is with outliers and high corruption of noise.

Artificial neural networks (ANNs) have been adopted for hyperspectral remote sensing processing [10]. Recently, as one of the very important technologies of ANNs, auto-encoder has attracted great attention in the hyperspectral community [11, 12]. Non-negative sparse auto-encoder (NNSAE) and denoising auto-encoder (DAE), as two special cases of auto-encoders, were employed to hyperspectral unmixing [11, 12, 13], with advanced denoising and intrinsic self-adaptation capabilities. However, as its strength is in the aspect of anti-noise, in case of outliers, it results in strong limitations. The presence of outliers can bring strong interference to its unmixing results, as outliers likely lead to initialization failure, which is essential for ANNs.

In this work, we develop a new approach based on the deep auto-encoder network (DAEN) aiming at tackling the outliers and low noise-signal-ratio in hyperspectral unmixing. The proposed method establishes a deep neural network based on auto-encoders, includes two main parts. First, we train a spectral model via stacked NNSAE, aiming at learning the spectral signatures such that to obtain a good initialization for the network. On the other hand, we adopt variational auto-encoder (VAE)[14] to perform blind unmixing for hyperspectral data.

The remainder of this paper is organized as follows. Section 2 introduces the proposed DAEN method. In section 3, the proposed approach is evaluated by using synthetic datasets, which allows us to conduct a quantitative comparison with other methods. Finally, section 4 concludes the paper with some remarks.

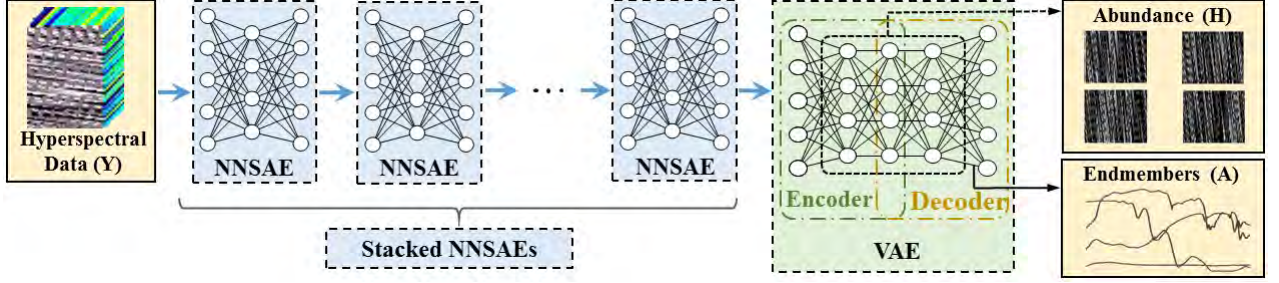


Fig. 1. The flowchart of the proposed DAEN.

## 2. PROPOSED APPROACH

In this section, we present the proposed DAEN for hyperspectral unmixing. As shown in Fig.1, which demonstrates the flowchart of the proposed approach, the proposed DAEN has two auto-encoders, i.e., the stacked NNSAEs for the learning of the spectral signatures, and a VAE for unmixing.

Following the linear spectral mixing model, this work assumes that the reflected spectra are linearly mixed by several endmembers. Hence, for a given observation  $\mathbf{y}_i \in \mathbb{R}^l$  with  $l$  being the number of bands, we have

$$\mathbf{y}_i = \mathbf{A}\mathbf{h}_i + \boldsymbol{\varepsilon}_i = \sum_{j=1}^m h_{ij}\mathbf{a}_j + \boldsymbol{\varepsilon}_i, \quad (1)$$

$$\text{s.t.: } \mathbf{h}_i \geq 0, \sum_{j=1}^m h_{ij} = 1,$$

where  $\mathbf{A} = [\mathbf{a}_1, \dots, \mathbf{a}_m] \in \mathbb{R}^{l \times m}$  is the endmember matrix with  $m$  being the number of endmembers,  $\mathbf{h}_i = [h_{i1}, \dots, h_{ij}, \dots, h_{im}]^T \in \mathbb{R}^m$  denotes the abundance fractions with  $h_{ij}$  corresponding to the  $j$ th endmember, and  $\boldsymbol{\varepsilon}_i$  is the noise vector. The two constraints  $\mathbf{h}_i \geq 0$  and  $\sum_{j=1}^m h_{ij} = 1$  are the abundance non-negativity constraint (ANC) and abundance sum-to-one constraint (ASC), respectively.

### 2.1. Non-negative Sparse Auto-Encoder (NNSAE)

In this work, we first run VCA  $k$  times, obtaining  $k \times m$  endmember candidates, which are then grouped into  $m$  sets based on the spectral angle distances (SADs). Let  $\mathbf{S}_j \in \mathbb{R}^{l \times k}$  be the training set of the  $j$ -th endmember, NNSAE uses  $\mathbf{S}_j$  to learn the reconstructed signature  $\hat{\mathbf{a}}_j$  as follows,

$$\hat{\mathbf{a}}_j = \mathbf{W}_j^{\text{output}} \mathbf{f}(\mathbf{W}_j^{\text{input}} \mathbf{S}_j), \quad (2)$$

where  $\mathbf{f}(\cdot)$  is an activation function,  $\mathbf{W}_j^{\text{input}} \in \mathbb{R}^{l \times l}$  is a matrix of weights from the input layer to the hidden layer and  $\mathbf{W}_j^{\text{output}} \in \mathbb{R}^{l \times l}$  is a matrix of connection weights between the hidden layer and the output layer. In practice, we share the weights between the input and hidden neurons with

those from hidden to output neurons, which means  $\mathbf{W}_j = \mathbf{W}_j^{\text{output}} = (\mathbf{W}_j^{\text{input}})^T$ , with  $T$  being matrix transposition. Therefore, problem (2) turns to,

$$\hat{\mathbf{a}}_j = \mathbf{W}_j \mathbf{f}(\mathbf{W}_j^T \mathbf{S}_j). \quad (3)$$

For the activation function  $\mathbf{f}(\cdot)$ , herein we adopt the logistic function as follows,

$$\mathbf{f}(\mathbf{g}_j) = \frac{1}{1 + \exp(-\mathbf{c}_j \cdot \mathbf{g}_j - \mathbf{d}_j)}, \quad (4)$$

where  $\mathbf{g}_j = \mathbf{W}_j^T \mathbf{S}_j$ ,  $\mathbf{c}_j$  and  $\mathbf{d}_j$  are parameters aiming at controlling the information transmission between neurons. Then, let  $\tau$  be the learning rate, and  $\varphi$  be a global parameter in the learning process controlling the mean activity level of the desired output distribution, we can use a gradient rule to update  $\mathbf{c}_j$  and  $\mathbf{d}_j$  as follows,

$$\begin{cases} \Delta \mathbf{d}_j = \tau(1 - (2 + \frac{1}{\varphi})\mathbf{f}_j + \frac{1}{\varphi}\mathbf{f}_j^2), \\ \Delta \mathbf{c}_j = \tau \frac{1}{\mathbf{c}_j} + \mathbf{g}_j \Delta \mathbf{d}_j, \end{cases} \quad (5)$$

where  $\tau$  and  $\varphi$  were empirically set as  $\tau = 0.0001$  and  $\varphi = 0.2$ , respectively [15].

With the aforementioned definition in hand, the learning reduces to the following update rule,

$$\Delta \mathbf{W}_j \leftarrow \eta \Delta \hat{\mathbf{a}}_j \mathbf{f}_j^T + |\mathbf{W}_j|, \quad (6)$$

where  $\Delta \hat{\mathbf{w}}_j$  is the gradient of endmember  $j$  for update,  $|\mathbf{W}_j|$  enforces the weight matrix to be non-negative,  $\eta$  is an adaptive learning rate[15]. In this work, following [15], we set  $\eta = \hat{\eta}(\|\mathbf{f}_j\|^2 + \epsilon)^{-1}$  with  $\hat{\eta} = 0.002$ , where  $\epsilon > 0$  is a small parameter to ensure the positivity of  $\eta$ .

### 2.2. Variational Auto-Encoder (VAE)

Following[14], let  $n$  be the number of pixel in the hyperspectral data,  $\mathbf{u}_i = [u_{i,1}, u_{i,2}, \dots, u_{i,m-1}]^T \in \mathbb{R}^{m-1}$  and  $\boldsymbol{\nu}_i = [\nu_{i,1}, \nu_{i,2}, \dots, \nu_{i,m-1}]^T \in \mathbb{R}^{m-1}$  be the reparameters of latent variables, for  $j = 1, \dots, m-1$ , we define  $h_{i,j} =$

$Cons(u_{i,j}, \nu_{i,j})$ , where  $Cons(\cdot)$  represents a decay function as follows,

$$Cons(u_{i,j}, \nu_{i,j}) = \begin{cases} u_{i,j} + \sigma \nu_{i,j}, & 0 < (u_{i,j} + \sigma \nu_{i,j}) < 1 \\ 0, & \text{otherwise} \end{cases} \quad (7)$$

where  $\sigma$  a parameter, following [6], which can be obtained via Monte Carlo (MC) sample. In order to meet the ASC, for  $j = m$ , we have  $h_{i,m} = 1 - \sum_{j=1}^{m-1} h_{i,m-1}$ .

Finally, with the aforementioned definition in mind, and let  $\mathbf{Y} = \{\mathbf{y}_1, \dots, \mathbf{y}_n\} \in \mathbb{R}^{l \times n}$ ,  $\mathbf{H} = \{\mathbf{h}_1, \dots, \mathbf{h}_n\} \in \mathbb{R}^{m \times n}$ , we define the following combinational objective function of VAE for unmixing,

$$(\mathbf{A}, \mathbf{H}) = \arg \min_{\mathbf{A}, \mathbf{H}} \frac{1}{2} \|\mathbf{Y} - \mathbf{A}\mathbf{H}\|_F^2 + \mu f_1(\mathbf{A}) + \lambda f_2(\mathbf{H}), \quad (8)$$

where  $\|\cdot\|_F^2$  denotes the Frobenius norm,  $\mu$  and  $\lambda$  are the parameters on two regularizers  $f_1(\mathbf{A})$  and  $f_2(\mathbf{H})$  on the mixing matrix and abundance fractions, respectively. In this work, we set  $f_1(\cdot) = \text{MinVol}(\mathbf{A})$ , aiming at enclosing all the pixels into the simplex constructed by the endmembers via minimum volume constraint [3]. On the other hand, employing the VAE, we define  $f_2(\mathbf{H})$  as,

$$f_2(\mathbf{H}) = \frac{1}{2} \sum_{i=1}^n \sum_{j=1}^{m-1} (1 + \ln u_{i,j}^2 - u_{i,j}^2 - \nu_{i,j}^2). \quad (9)$$

Problem (9) is combinational and non-convex, which is difficult to optimize. In this work, we propose an iterative scheme to optimize  $\mathbf{A}$  and  $\mathbf{H}$  respectively, both of which are solved by a gradient descent method [16].

### 3. EXPERIMENTAL RESULTS

The effectiveness of the proposed DAEN is evaluated by using synthetic data. The data are generated according to a linear mixing model with 676 pixels with maximum abundance purity of 0.8. The data set has 4 endmembers (the pure spectral signatures), with 224 spectral bands covering the spectral range from 0.4  $\mu\text{m}$  to 2.5  $\mu\text{m}$ , are randomly selected from the USGS library. As the main target of the proposed approach is low SNR, the synthetic data is then corrupted by 20dB white Gaussian noise. Finally, two scenarios, i.e., no outlier and 5 outliers, are considered for the experiments.

In this paper, three indicators, i.e., spectral angle distance (SAD), reconstruction error (RE), and root mean square error (RMSE) are used to assess the accuracy of the unmixing results, which are given as follows,

$$\begin{cases} \text{SAD}[\mathbf{a}_j, \hat{\mathbf{a}}_j] = \arccos\left(\frac{[\mathbf{a}_j, \hat{\mathbf{a}}_j]}{\|\mathbf{a}_j\| \|\hat{\mathbf{a}}_j\|}\right), \\ \text{RE}(\{\mathbf{y}_i\}_{i=1}^n, \{\hat{\mathbf{y}}_i\}_{i=1}^n) = \frac{1}{n} \sum_{i=1}^n \sqrt{\|\mathbf{y}_i - \hat{\mathbf{y}}_i\|_2^2}, \\ \text{RMSE}(\hat{\mathbf{h}}_i, \mathbf{h}_i) = \frac{1}{n} \sum_{i=1}^n \sqrt{\|\mathbf{h}_i - \hat{\mathbf{h}}_i\|_2^2}, \end{cases}$$

where  $\hat{\mathbf{a}}_j$  and  $\mathbf{a}_j$  are the extracted endmember and the library spectrum,  $\hat{\mathbf{y}}_i$  and  $\mathbf{y}_i$  are the reconstruction and observation of pixel  $i$ ,  $\hat{\mathbf{h}}_i$  and  $\mathbf{h}_i$  are the corresponding estimated and actual abundance fractions, respectively.

Table 1 reports the obtained results. Comparisons with several widely used unmixing algorithms, including N-FINDR[1], VCA[2], MVC-NMF[3], Bayesian approach [6], PCOMMEND[7], and ASNSA[11], are reported. It can be observed that the proposed DAEN obtained the best results, which are much better than those provided by the other methods.

**Table 1.** The average SADs (in radians), REs and RMSEs along with their standard deviations obtained from 10 Monte Carlo runs by different methods for the considered simulated data. Best results are in bold.

Method	SAD	RMSE	RE
No outlier			
N-FINDR	0.0608	0.5745	0.0482
VCA	0.0556	0.5833	0.0465
MVC-NMF	0.0090	0.5397	0.0279
Bayesian	0.0182	0.4904	0.0363
PCOMMEND	0.0379	0.5110	0.0249
ASNSA	0.0293	0.5087	0.0414
DAEN	<b>0.0069</b>	<b>0.4619</b>	<b>0.0226</b>
5 outliers			
N-FINDR	0.2012	0.7024	0.0550
VCA	0.1758	0.5790	0.0481
MVC-NMF	0.1194	0.5705	0.0523
Bayesian	0.1905	0.5937	0.0558
PCOMMEND	0.2169	0.6613	0.0307
ASNSA	0.0372	0.5016	0.0324
DAEN	<b>0.0105</b>	<b>0.4723</b>	<b>0.0284</b>

For illustrative purposes, Fig.2 shows the unmixing results obtained by the proposed DAEN and the other methods, for the problem with 5 outliers. It can be further seen that the proposed DAEN achieved very promising results.

### 4. CONCLUSIONS AND FUTURE LINES

In this paper, we propose a deep auto-encoder network (DAEN) for hyperspectral unmixing, which includes a stack and multi-hidden-layers of nonnegative sparse auto-encoders to initialize the endmember signatures and a variational auto-encoder to perform unmixing, achieving the mixing matrix and the abundance fractions. By taking advantage from the auto-encoders, the proposed DAEN can handle problems with

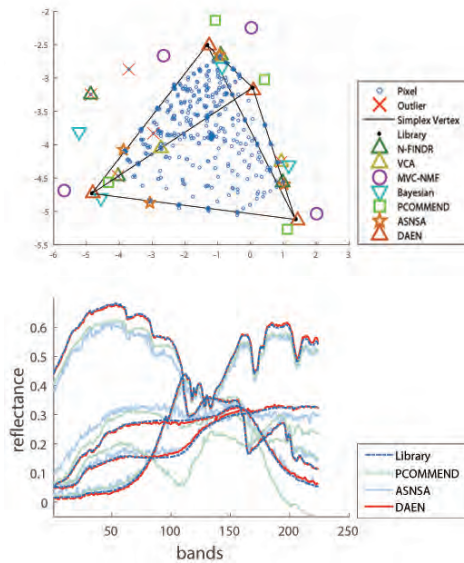


**Fig. 2.** Graphical results from the proposed DAEN and the other methods. Top: scattering plot for the consider synthetic data with 5 outliers. Bottom: the obtained endmember signatures and their references from USGS library.

outliers and low signal to noise ratio. Future work will be focused on a more exhaustive evaluation of the method with real hyperspectral data sets.

## 5. REFERENCES

- [1] M. E. Winter, "N-FINDR: An algorithm for fast autonomous spectral endmember determination in hyperspectral data," in *Proc. SPIE Image Symposium V*, vol. 3753, pp. 1–10, Oct. 1999.
- [2] J. M. P. Nascimento and J. M. Dias-Bioucas, "Vertex component analysis: A fast algorithm to unmix hyperspectral data," *IEEE Trans. Geosci. and Remote Sens.*, vol. 43, no. 4, pp. 898–910, Apr. 2005.
- [3] L. Miao and H. Qi, "Endmember extraction from highly mixed data using minimum volume constrained non-negative matrix factorization," *IEEE Trans. Geosci. and Remote Sens.*, vol. 45, no. 3, pp. 765–777, Mar. 2007.
- [4] J. Li, A. Agathos, D. Zaharie, J. M. Bioucas-Dias, A. Plaza, and X. Li, "Minimum volume simplex analysis: A fast algorithm for linear hyperspectral unmixing," *IEEE Trans. Geosci. and Remote Sens.*, vol. 53, no. 9, pp. 5067–5082, 2015.
- [5] J. Li, J. M. Bioucas-Dias, A. Plaza, and L. Liu, "Robust collaborative nonnegative matrix factorization for hyperspectral unmixing," *IEEE Trans. Geosci. and Remote Sens.*, vol. 54, no. 10, pp. 6076–6090, 2016.
- [6] N. Dobigeon, S. Moussaoui, M. Coulon, J. Y. Tourneret, and A. O. Hero, "Joint bayesian endmember extraction and linear unmixing for hyperspectral imagery," *IEEE Transactions on Signal Processing*, vol. 57, no. 11, pp. 4355–4368, Nov. 2009.
- [7] A. Zare, P. Gader, O. Bchir, and H. Frigui, "Piecewise convex multiple-model endmember detection and spectral unmixing," *IEEE Trans. Geosci. and Remote Sens.*, vol. 51, no. 5, pp. 2853–2862, Nov. 2013.
- [8] X. Lu, H. Wu, Y. Yuan, P. Yan, and X. Li, "Manifold regularized sparse nmf for hyperspectral unmixing," *IEEE Trans. Geosci. and Remote Sens.*, vol. 51, no. 5, pp. 2815–2826, 2013.
- [9] J. M. Bioucas-Dias, A. Plaza, N. Dobigeon, M. Parente, Q. Du, P. Gader, and J. Chanussot, "Hyperspectral unmixing overview: Geometrical, statistical, and sparse regression-based approaches," *IEEE J., Sel. Topics Appl. Earth Observ. and Remote Sens.*, vol. 5, no. 2, pp. 354–379, Apr. 2012.
- [10] J. Plaza and A. Plaza, "Spectral mixture analysis of hyperspectral scenes using intelligently selected training samples," *IEEE Geosci. Remote Sens. Lett.*, vol. 7, no. 2, pp. 371–375, Apr. 2010.
- [11] Y. Su, A. Marinoni, J. Li, A. Plaza, and P. Gamba, "Nonnegative sparse autoencoder for robust endmember extraction from remotely sensed hyperspectral images," *2017 IEEE International Geoscience and Remote Sensing Symposium (IGARSS)*, pp. 205–208, Jul. 2017.
- [12] Y. Qu, R. Guo, and H. Qi, "Spectral unmixing through part-based non-negative constraint denoising autoencoder," *2017 IEEE International Geoscience and Remote Sensing Symposium (IGARSS)*, pp. 209–212, Jul. 2017.
- [13] R. Guo, W. Wang, and H. Qi, "Hyperspectral image unmixing using autoencoder cascade," *IEEE GRSS Workshop Hyperspectral Image Signal Process.: Evolution in Remote Sens.(WHISPERS)*, pp. 1–4, Jun. 2015.
- [14] D. P. Kingma and M. Welling, "Auto-encoding variational bayes," Dec. 2013.
- [15] A. Lemme, R. F. Reinhart, and J. J. Steil, "Online learning and generalization of parts-based image representations by non-negative sparse autoencoders," *Neural Networks*, vol. 33, pp. 194–203, May. 2012.
- [16] M. D. Zeiler, "Adadelata: An adaptive learning rate method," *Computer Science*, Dec. 2012.